State of Stress in Strain Wave Gear Flexspline Cup on Insertion of Drive Cam - Experiment and Analysis

Vineet Sahoo, and Rathindranath Maiti

***Abstract* - Stresses developed in the very thin walled flex - gear cup of Harmonic drive on insertion of the conventional oval shaped wave generator cam and circular spline unassembled, are analysed using FEM in Ansys® environment. To estimate the stresses in the thin wall and more importantly on the bottom flange of the cup, strains at different locations of the cup are measured, keeping the cup fixed and rotating the cam inside the cup. The experimental results have good agreement with the FEA results. The initial torque required to rotate the cam inside the flex-gear cup without the circular spline assembled, is estimated. It is also verified experimentally.**

***Index Terms* - Experimental technique, Harmonic Drive, Initial torque loss, Load distribution, Wave generator cam insertion,**

I. INTRODUCTION

The Harmonic Drive (HD) (or Strain Wave Gearing (SWG) [1]) is a unique single stage high transmission ratio gear unit, used in many fields such as in motion control of antenna of solar array drive, in industrial robots, and in medical robots and equipments etc. As shown in Fig 1, an HD consists of a flexspline (FS) or a flex gear (FG) (in this paper, the term FG is used), a circular spline (CS) or a ring gear (RG) (in this paper, the term RG is used), and an oval shaped strain wave generator (SWG) cam assembly. The most crucial part, the cup shaped FG, is a thin walled cup shaped component and flex gear at the free end of cup, is a thin rimmed gear with backup ratio (rim thickness: tooth height) even less than one. Usually the output motion is taken from one of the gears keeping the other one fixed. The operational and kinematic details are well-established [1-5]. Some inherent dynamics is also known [6], that perhaps cannot be ignored.

During motion, the body of the FG cup experiences alternating stress due to flexion. Therefore, examining the strength of the FG cup in such fatigue loads is essential in the design process. Secondly, considering the control aspect and performance, it is also essential to estimate the zero load initial torque required to flex the FG cup due to cam rotation.

Several research results are reported [7-10] on the strength basis design of the FG cup alone. However, investigations on the pattern of the FG and RG teeth contacts, considering stress distribution on thin rim flex-gear, still attract researchers for coming up with more general solutions.

Manuscript received Feb 15, 2016; revised Apr 06, 2016.

Vineet Sahoo, Doctoral Student, Indian Institute of Technology Kharagpur, Kharagpur, West Bengal, India-721302; +918348502799; email: vineet.sahoo@mech.iitkgp.ernet.in,

Rathindranath Maiti, Professor, Indian Institute of Technology Kharagpur, Kharagpur, West Bengal, India-721302; +919434065298; email: rmaiti@mech.iitkgp.ernet.in,

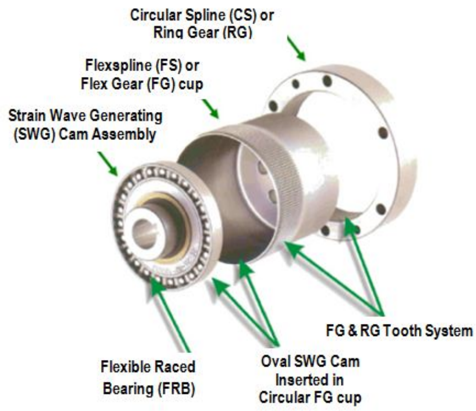

Fig 1. Basic Components of a Harmonic Drive.

In the present investigation an attempt is made to determine stress distribution patterns in the FG cup, the most critically stressed component in HDs, due to the effect of insertion of the SWG cam and its rotation, without the RG assembled, and thereby without any applied load. FEM is adopted in order to estimate the stresses developed in the FG cup due to the insertion of the wave generator cam and to realize the contact between FRB outer race and the FG cup's inner surface. Experiments are conducted and strains at several key places of the inner and outer surfaces of the FG cup are measured. Stresses are then calculated using measured strains, and compared with FEM results. The torque required to rotate the SWG cam deflecting the FG cup continuously with its angular motion, is also estimated. This no load torque loss may help in developing the motion control system.

II. STRESSES IN FG CUP DUE TO SWG CAM INSERTION

A. Finite Element Approach

First, a solid model of the FG cup, along with the inserted oval shaped SWG cam, is developed. For the purpose of FEM modelling, the oval shaped cam is divided into two equal parts (Fig 2), by removing a strip of thickness equal to twice the centre distance between the FG and RG, when FG is at circular shape. The two parts are now gradually pushed apart to restore the original outer shape of the cam, inside the FG cup and below the flex gear. This would cause FG teeth mesh with RG teeth at two places 180^{o} apart, if the FG cup is now axially pushed inside RG. FEM in Ansys® environment automatically estimates stresses in the FG cup due to the cam, both of which are elastic bodies.

Assuming that there is no centre distance correction, the centre distance is formulated as:

$$A = m\frac{Z_g - Z_p}{2} \quad (1)$$

Where, A- nominal centre distance, m= module, Z_g - no. of teeth in RG, and Z_p - no. of teeth in FG.

Therefore, the semi major axis 'a' of the oval FG can be expressed as:

$$a = r_p + A \quad (2)$$

In case of unmodified gear which is:

$$a = r_p + A = m\left(\frac{Z_p}{2} + \frac{Z_g - Z_p}{2}\right) = m\frac{Z_g}{2} \quad (3)$$

TABLE I
Gear Parameter.

Description	Flex-Gear(FG)	Circular Gear(CG)
No. Of Teeth	Z_p=156	Z_g=158
Pressure Angle	30 deg	
Module	0.529 mm (48 DP)	
Addendum Factor	0.8	0.8
Dedendum Factor	1.25	1.25
Centre Distance	0.529 mm	
Material	Steel (EN24)	
Oval SWG Cam (Assembled with FRB)		
Major Axis	80.85 mm	
Minor Axis	78.66 mm	

.

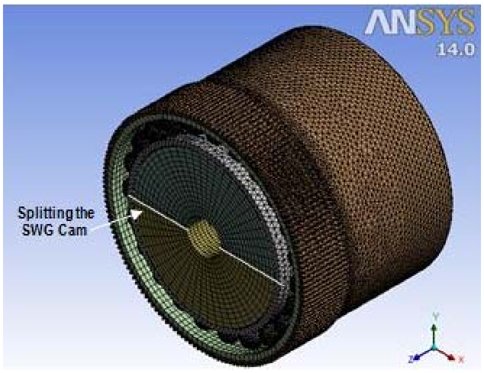

Fig 2. Finite Element Meshed Model for FG cup and SWG Cam Assembly.

Components of typical commercially available HD units, having the nominal data and specification as detailed in Table 1, are considered for FEM analysis and experiments. Fig 2 shows the meshed model of FG cup together with the assembled SWG cam. The major axis of the oval SWG cam lies on the vertical axis (i.e. Y-axis). In solid modelling, SOLID187 elements are used. Contact pairs are modelled with CONTA174 and TARGE170. The materials are structural steel for all parts.

All the degrees of freedom at surfaces at the closed end of the FG cup are constrained. As mentioned earlier, the two divided parts of SWG cam are given the displacements along the Y axis of +0.529 mm (equal to centre distance as in Table 1) for upper one and -0.529 mm for the lower one.

FEA results are illustrated in Fig 3. As the FG cup experiences stretching in circumferential direction and bending in longitudinal direction, the von-Mises stresses are estimated. It is observed that the bearing outer race experiences maximum stress. This is due to high contact stress. However, in FG cup, the combined maximum stress is 124 MPa (Fig 3b) at the contact zone of the bearing outer race and FG cup inner surface. The maximum stress on the cup outer wall surface is much lesser at 42 MPa. The stress due to bending occurs at the bottom flange of the FG cup. The magnitude of stress is around 100 MPa (Fig 4). For deformation analysis, the applied deformation on elliptical cam is 0.529 mm, but maximum deformation in cup open end is 0.55 mm with no load. It is to be noted that the maximum deformation occurs not at the edge of FG cup end but at the contact point of the outer race of the bearing and the inner surface of FG, inside of cup. This is due to the coning of the FG cup, which is unavoidable.

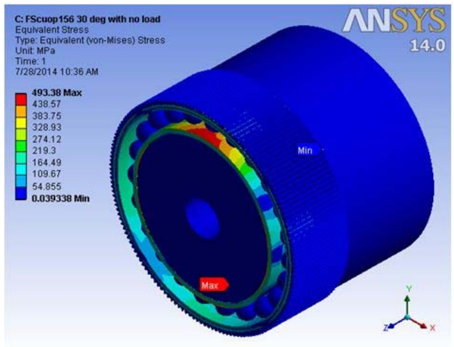

(a). von-Mises stress on assembly of FG cup and Wave Generator

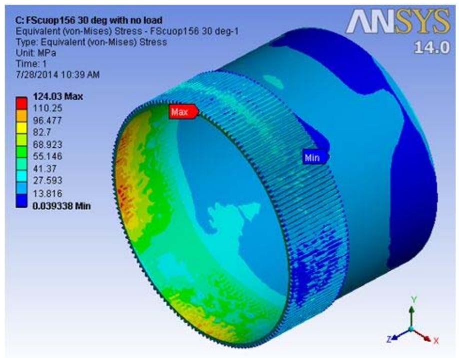

(b). von-Mises stress on FG cup inner surface.
Fig 3. Ansys® Simulation Results.

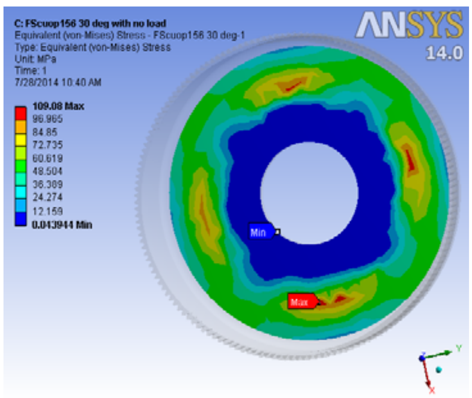

Fig 4. von-Mises stress on bottom flange surface of FG cup.

ISBN: 978-988-14048-0-0
ISSN: 2078-0958 (Print); ISSN: 2078-0966 (Online)

B. Experimental Approach

Strains are measured at different circumferential positions on inside and outside surfaces of the FG cup wall and the bottom flange as the SWG cam, inside the cup, is rotated. Stresses at those places are calculated using standard techniques. Thus the stress map of the full FG cup is established on the cam insertion. The details of the experimental techniques are described in subsequent sections.

Experimental Techniques

Strain gages are fixed on the inner and outer surfaces of the FG cup along global X and Y axes fixed to the cup as shown in Figs. 5. These strain gages are connected to a strain measuring unit and a strain indicator (Vishay Instrument, SB 10 & 3310 Strain Indicator). Here, 120 ohm strain gages are used to measure the strains and a quarter bridge circuit is used to measure the strain for each strain gage. Note that no strain gage could be use for the direct measurement of strains along the radial direction of the thin walled portion of the FG cup bottom flange as the annular section is narrow (see Fig 5(b)). The strains in the radial direction are calculated using Poisson's ratio.

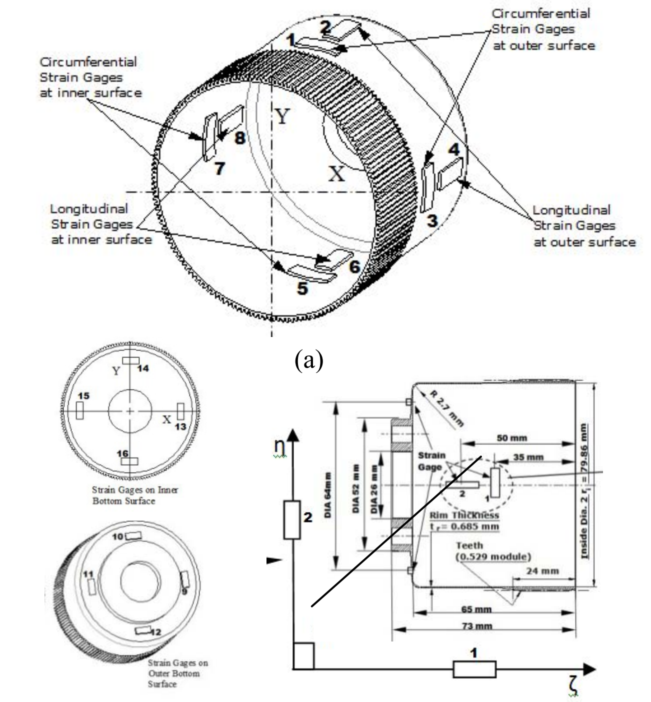

Fig 5. Strain gages fixed on FG cup inside and outside wall and end flange.

Figure 6(a) shows variation in strains recorded experimentally as well as by FEA at the outer surface of the FG cup wall in the circumferential diection at the gage 3 on the X axis and at gage 1 on the Y axis. Figure 6 (b) shows strains on the inner surface of the FG cup wall. Similarly, variations in strains in the longitudinal direction are also obtained. Experimental results have good agreement with theoretical (FEA) estimates. Stresses are calculated using standard techniques in the considered sections based on strains in the respective sections where strain gages are fixed (see Fig 5(c)). Sample results are shown in Fig 7.

Experimental results are close to theoretical estimates for one full rotation of the cam for the particular sections where strain gages are placed (Fig 5). Therefore, it can be assumed that the FEA stress results based on the proposed finite element model can be used for the design and any relevant pupose for the whole FG cup.

Next the principal stresses are calulated to locate where maximum stresses (tensile and compressive) occur. Some sample stress results, estimated based on obtained strain records by experiments and FEA for the outer surface of the FG cup wall are presented in 3D views (Fig 8).

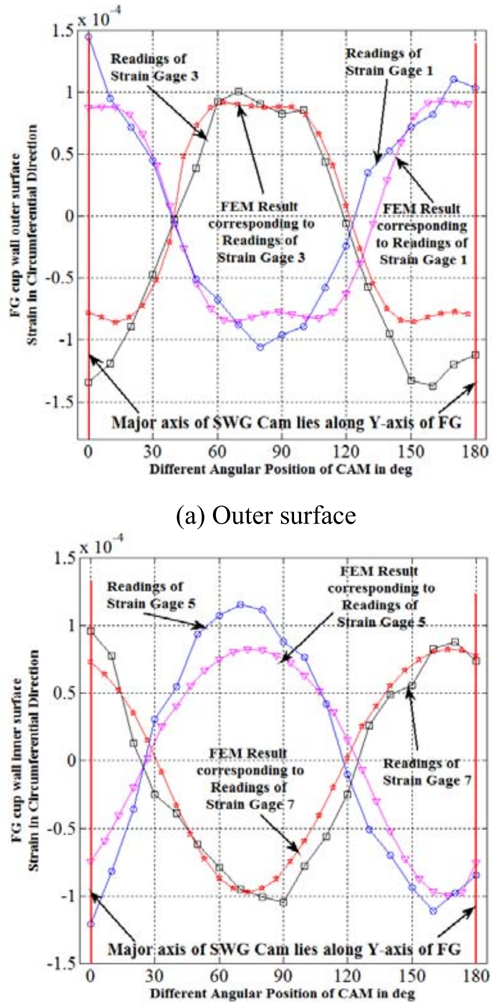

Fig 6. Variation in strains in circumferential direction in FG cup wall, with cam rotation.

C. Estimation of Stress on FG cup Bottom Flange Surface at the close end

The FG cup closed end flange experiences bending when the SWG cam is inserted. To measure the strains at the bottom inner and outer surfaces, the strain bridge (quarter) is formed with strain gages 9 through 12 on the bottom flange outer surface, and 13 through 16 on the bottom flange inner surface (Fig 5b). On both inner and outer surfaces, strain gages are placed in tangential direction. Experiments are carried out for half rotation i.e., 180 degree rotation of the SWG cam (as there are two identical contact zones at the two vertices of the major axis) to get the stresses at a point for all positions of the SWG cam. The acquired strain results are compared with FEM estimated results, as shown in Fig9.

ISBN: 978-988-14048-0-0
ISSN: 2078-0958 (Print); ISSN: 2078-0966 (Online)

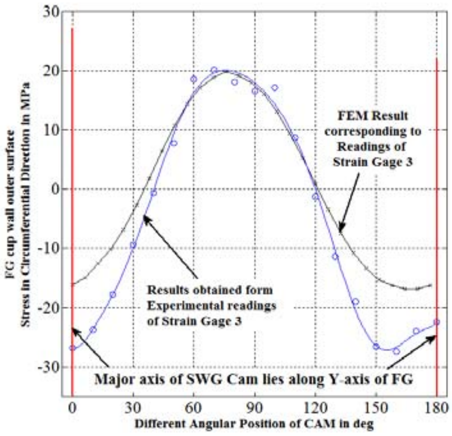

(a) Outer surface

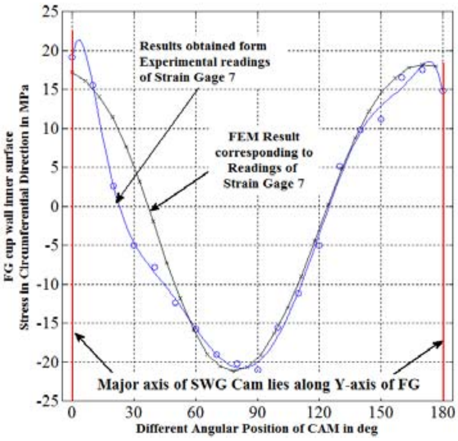

(b) Inner surface

Fig 7. Variation in stresses in circumferential direction in FG Cup wall, with cam rotation.

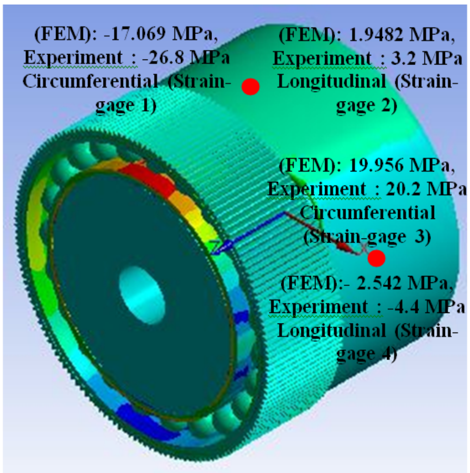

Fig 8. Stresses at different locations of FG cup.

Considering the bottom flange as a thin plate or diaphragm the maximum tangential strain (in elongation) in the outer surface of the FS flange (at strain gage 10, Fig 5) recorded experimentally, is about 79 micron, averaging the values, when the SWG cam's major axis is at 0^{o} position and again identical after 180^{o} rotation (Fig 9). By FEA, the average value is about 52 micron. Maximum strains (in contraction) when the cam rotates by 90^{o} are -57 and -65 microns by experiment and FEA respectively. Otherwise, results obtained by FEA and experiments have good agreement. Similarly, in the recorded maximum strains at the strain gage 14 (Fig 5), inside the flange at the same place where the gage 10 is at outside, are about -79 micron (average) by experiment and -39.5 micron (average) by FEA for cam's 0^{o} it and after 180^{o} positions. For 90^{o} rotation, the strains (in elongation) are 62 micron and 47 micron (Fig 9) respectively.

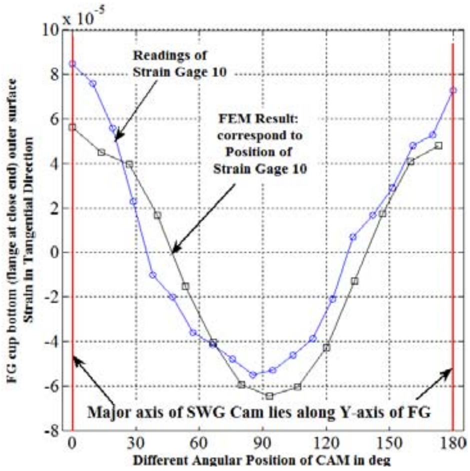

Fig 9. Variation in strains in circumferential/tangential direction in FG cup flange outer surfaces, with cam rotation (Experiment and FEA).

The bending stresses (acting in the radial direction in the FS flange), are now estimated from the experimental data. First, strains in radial direction are estimated using Poisson ratio. It is to be noted that (as mentioned earlier) no strain gage could be placed on the FG cup flange in its radial direction due to space problem. As there is no load in the circumferential direction (no applied torque) the strains in radial direction is directly calculated from the experimental strain values in circumferential i.e., tangential direction. The sample results are plotted in Fig 10.

As in Fig 10, the maximum bending stress (tensile) in the bottom flange outer surface is 36.7 MPa by experiment and 35.75 MPa by FEA occur at the position of gage 10 when the cam's minor axis passes through it. Similarly, for other positions results were obtained. Relatively higher differences in results by experiment and FEA for some positions may be due to some error in measurement or the assigned boundary conditions in FEA.

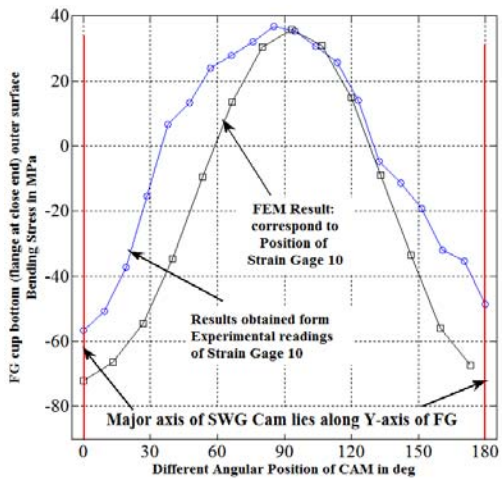

Fig 10. Variation in stresses (in bending) at outer surface of FG cup flange at close end.

As observed, the stresses at the flange along the minor axis are higher than those are along the major axis. When the load is applied i.e., torque is transmitted the resultant stress will increase, but the increment will be more or less same everywhere in the flange. The loads at teeth contacts will not have much effect on the stresses along the major axis and no effect along the minor axis.

Next to get the overall stress map in the FG cup variation in stresses in the FG cup wall and flange, due to cam incursion and its rotation, are plotted together for comparison, as shown in Fig 11. The stresses in the wall are very less in comparison to the flange stresses. It is apparent that the flange, near the hub along the mirror axis, will experience the highest alternating stresses and prone to fatigue failure.

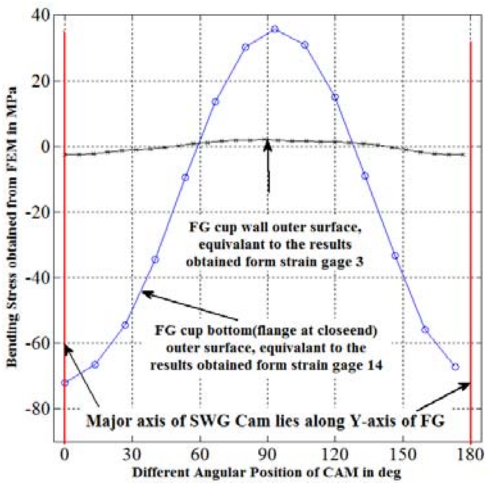

Fig 11. Variation in maximum stresses (in bending) on FG Cup wall and bottom flange outer surface due to SWG cam insertion only.

III. LOAD DISTRIBUTION ON THE OUTER RACE OF THE FRB DUE TO INSERTION OF SWG CAM INSIDE FG CUP

As mentioned earlier in FEM modelling, the deflection of the FG cup is gradually given by moving the two equal halves of the cam, along the major axis to the final position. In FEA, due to such deflection of the cup, the loads are assigned to the nodes automatically and strains are generated in all elements. Now for estimating the radial loads acting on the FRB, following model is considered.

For simplicity in analysis, first of all the assembled SWG cam is replaced by an assumed parabolic distributed force system along the contact zone of SWG cam and flex-gear cup, following the model proposed by Lee and Shen [11] and Sentoku et al. [12]. Initially an arbitrary active (load transmitting) contact zone between SWG cam and flex-gear inner cup surface is assumed as shown in Fig 12(a). The angle subtended by the contact zone at the centre of flex-gear is the 'angle of contact zone' defined by ϕ_1. The middle/maximum value of the parabolic loading lies on the major axis of nearly elliptically deflected flex-gear. However, the contact of the FG cup inner surface with the outer race of the FRB along its width occurs at the inner end along major axis due to coning effect. Apparently, the contact gradually shifts towards the outer end of the bearing as the contact progresses from major axis to minor axis. In the present analysis, this contact is considered a line contact and for the active contact zone, it is on the inner edge of the FRB outer race, as the zone is small in comparison to the outer periphery of the FRB outer race.

In the finite element model, now the parabolic loading is applied. The magnitude of the applied loading at different points within the contact zone is based on the eq. (4).

$$q = \frac{4q_0(\theta-\phi_2)}{\phi_1^2}\left\{\left(\phi_1+\phi_2\right)-\theta\right\} \qquad (4)$$

Where θ= angle at any section from positive x- axis.

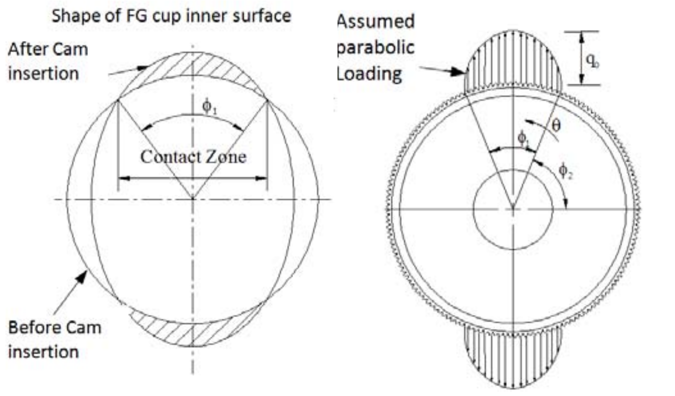

(a). Contact Zone between FS and SWG cam

(b). Loading on FG cup inner surface

Fig 12. Loading on flex-gear along the contact zone due to insertion of SWG cam.

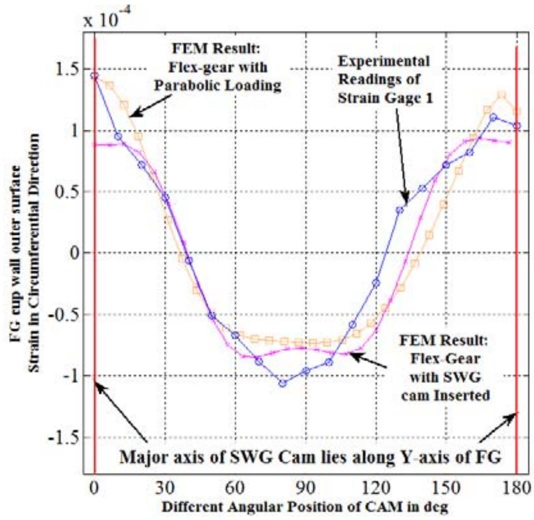

Fig 13. Variation in strain distribution pattern with parabolic loading-comparison with results in Fig 6(a).

To get the probable parabolic load distribution q_0 value is varied randomly, and the strains in FG cup are obtained in FEA until the stains results both in magnitude and pattern matches or becomes close to the strains obtained from the experimental investigation and FEM results as shown in Fig 7(b). Thus, the best possible q_0 value is obtained. With a few trails, q_0 obtained for the considered FG cup and SWG cam is 18 N. The results along with FEA results with cam insertion model and experiment are plotted in Fig 12. As the results are very close to each other, the parabolic distributed equivalent load pattern is considered as the load on the FRB of the cam.

ISBN: 978-988-14048-0-0
ISSN: 2078-0958 (Print); ISSN: 2078-0966 (Online)

IV. INITIAL NO-LOAD TORQUE LOSS DUE TO SWG CAM ROTATION

As the FG cup is strained due to the SWG cam insertion, some amount of torque must be required to rotate the cam even at no load (and without the ring gear assembled). The loads at different balls of FRB are obtained from above mentioned parabolic loading. This parabolic loading creates vertical point loads at the contact points of balls and outer race of FRB, which in-turns generate rolling frictional force. This rolling frictional force is generating a torque at the centre of FRB. This torque is the initial torque loss (i.e. torque loss before application of load) due to insertion of SWG cam. Estimation of this initial torque is required for setting motion control of such units. Referring to the Fig 13, the amount of torque may be estimated as follows.

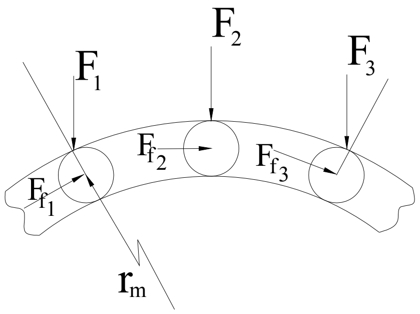

Fig 13. Loads acting on FRB
(assembled SWG cam inside the FG cup).

F_i is the load transmitted from flex-gear to bearing surface of wave generator

F_{fi} is the rolling frictional force at mean radius r_m.

μ_r is the coefficient of rolling friction

Hence, the initial torque loss is obtained as:

$$\text{Torque, } T = \mu_r r_m x \sum F_i \qquad (5)$$

In the present study of mentioned harmonic drive unit, the balls of FRB are not so rigid. The balls are quite free to move inside the inner and outer race of FRB. For that reason, the coefficient of rolling friction is considered as 0.2. With the obtained q_0 value as 18 N, the torque is formulated as 1.5795 N-m.

V. CONCLUSION

First the stress distribution pattern in the flex gear cup is investigated using finite element techniques. This is the most critically stressed component in HDs, due to the effect of insertion of the SWG cam and its rotation without the RG assembled. The FEA results at a few sections of the FG cup wall and at one circumferential section are verified by experiments. It is found that the maximum bending stress develops at the bottom flange, in the transverse direction of the position of major axis of the cam. As the location is subjected to this stress in alternating manner, fatigue failure may result. With the applied torque, the mean stress will increase. In designing the FG cup, this section must be optimized, keeping the FG cup flexible. Apart from this section, the thin cup wall adjacent to the teeth contacts (at the tips of major axis of the SWG cam) experience high stress. In addition, the flexible outer race of the bearing of the SWG cam experiences high stress. As the FG cups of HDs have more or less similar shapes, the proposed FEA can be used to design and analyze stresses due to insertion of cam.

Next, the torque required to rotate the SWG cam, deflecting the FG cup continuously with its angular motion, is also estimated. This no load torque loss, although small in comparison with torque transmitting capacity, helps in developing motion control algorithms and performing design optimization for such units.

ACKNOWLEDGMENT

This research work is an outcome of the general PhD programme in the authors' Institute, IIT Kharagpur, India. There is no specific financial grant for this investigation. However, the project grant to Maiti and Ray [5], from DST India, is deeply acknowledged.

REFERENCES

[1] C. W. Musser, Breakthrough in mechanical drive design: the harmonic drive, Mach Des 14 (1960) 160–172.
[2] B. Routh, R. Maiti, A. Sobczyk, A. K. Ray, An investigation on secondary force contacts of tooth pairs in conventional harmonic drives with involute toothed gear set. Proceedings of IMechE (UK), Journal of Mechanical Engineering Science, Part C (in Press) 2015; DOI: 10.1177/0954406215577983.
[3] R. Maiti, I. Biswas, V. Nema, S. Basu, B. S. Mahanto, B. Routh, Design and development of strain wave generating cam for a new concept 'Harmonic Drive'. Proceedings of IMechE (UK), Journal of Mechanical Engineering Science, Part C. 227(8) (2013) 1870-1884.
[4] R. Maiti, A Novel Harmonic Drive with Pure Involute Tooth Gear Pair. *ASME Journal of Mechanical Design*. 126(1) (2004) 178-182.
[5] R. Maiti, M. C. Ray, Design, Development and Performance Study of a New Concept Harmonic Drive," Project (Ref. SR/S3/RM-04/2002,11-07-2002 of DST, Govt. of India) Completion report, 2005.
[6] T. D. Tuttle, Understanding and Modeling the Behavior of a Harmonic Drive Gear Transmission. Technical report, MIT Artificial Intelligence Laboratory 1992.
[7] K. Oguz, E. Fehmi, Shape Optimization of Tooth Profile of A Flex-spline for a Harmonic Drive by Finite Element Modeling, Materials and Designs 28 (2007) 441-447.
[8] W. Ostapski, I. Mukha, Stress State Analysis of Harmonic Drive Elements by FEM, Bulletin of the polish academy of sciences 55(1) (2007) 115-123.
[9] C. Zou, T. Tao, G. Jiang, X. Mei, Deformation and Stress Analysis of Short flex-gear in the Harmonic Derive System with Load, In: IEEE International Conference on Mechatronics and Automation (ICMA), Takamatsu, Japan, 4-7 Aug. 2013, 676-680.
[10] M. Kikuchi, R. Nitta, Y. Kiyosawa, Stress Analysis of Cup Type Strain Wave Gearing, Key Engineering Materials 243-244 (2003) 129-134.
[11] K. Le, Y. Shen, Analysis method of bearing loads distributed on wave generator of a harmonic drive device, Mechanical Science and Technology for Aerospace Engineering. 34(2) (1990) 38-45.
[12] H. Sentoku, T. Satou, Y. Kiyosawa, X. Zhang, Characteristics of load transmission in strain wave gearing (1st Report, Derivation of load distribution on tooth flank), Trans. Japanese Society of Mechanical Engineering, 70(696) (2004) 2515-2522.

ISBN: 978-988-14048-0-0
ISSN: 2078-0958 (Print); ISSN: 2078-0966 (Online)